9th European Workshop on Structural Health Monitoring
July 10-13, 2018, Manchester, United Kingdom

Comparison of damage sensitivities of autoregressive coefficients and natural frequencies for structural health monitoring of a top tensioned riser

Bugra Bayik[1], Piotr Omenzetter[1,2], Dominic van der A[1] and Ekaterina Pavlovskaia[1,3]
1) School of Engineering, University of Aberdeen, Aberdeen AB24 3UE, UK
2) The Lloyd's Register Foundation Centre for Safety and Reliability Engineering, University of Aberdeen
3) Centre for Applied Dynamics Research, University of Aberdeen

Abstract

Risers are important components of offshore oil extraction facilities as they connect the surface structure to a pipeline or well-head on the seabed to transport hydrocarbons between the two. Damage incidents in risers may lead to catastrophic economic, environmental and human safety consequences. To avoid the disastrous outcomes of such incidents, early detection of damage in risers is of paramount importance and vibration-based structural health monitoring (SHM) is a promising means of achieving this. Although vibration-based SHM has been extensively studied for several types of structures and systems such as rotating machinery, aerospace structures, bridges and wind turbines, its application to risers has hardly been explored to date. In this paper, application of vibration-based SHM to a top tensioned riser is investigated. To that end, an analytical distributed parameter model is formulated using the Galerkin method and dynamic response of the riser to ambient surface wave excitations is obtained at the healthy and damaged states. Corrosion damage is considered here as it is the predominant cause of damage incidents in risers and it is modelled as cross-sectional area loss at the damaged portion of the riser. To represent the wave excitations realistically, energy density distribution of the sea states is obtained from the JONSWAP wave spectrum. Finally, from the dynamic response of the riser, auto-regressive coefficients and riser natural frequencies are identified and their damage sensitivities are compared for a series of damage extents.

1. Introduction

Top-tensioned risers (TTRs) are slender pipes which connect an offshore surface structure to the seabed and transport products between the two. They operate in a corrosive marine environment under significant wave and current environmental loads and hence are exposed to several damage mechanisms. In the PARLOC 2001 report [1], damage statistics are presented for steel risers operating in the North Sea from 1975 to 2001, and corrosion damage is shown to be the predominant cause of past damage incidents. The methods used for corrosion inspection in risers, such as visual inspection, ultrasonic techniques, acoustic emission and infrared thermography, are reviewed by Lozev et al [2] and evaluated as having limited potential due to clean surface and complex equipment

requirements, high costs, and their ability to detect only specific types of corrosion damage. Moreover, most of these methods can be applied only periodically at predetermined time intervals and they are effective only locally and hence require prior knowledge of the approximate damage location for an economically and practically viable application. Allowing for globally effective and continuous inspection, vibration-based structural health monitoring (SHM) methods are promising for detection of corrosion damage in risers. However, their potential for risers, and similar systems such as pipelines, has hardly been explored to date.

Several studies applied modal parameters-based damage sensitive features (DSFs) to vibration-based SHM of risers and pipelines. Zhou et al. [3] used the transfer matrix method and obtained mode-shape curvatures of a riser for damage localization. Huang and Nagarajaiah [4] proposed application of a time-frequency domain blind identification method for identification of modal properties from vortex induced vibrations of a deep-water riser. As an alternative to modal parameters-based DSFs, several authors fitted parametric time series models to dynamic response of risers and utilized these models for damage identification. Bao et al. [5] used an auto-regressive moving average (ARMA) model for detecting damage in pipelines on the seabed. Similarly, Liu et al. [6] used an ARMA model for damage localisation in a TTR subject to white noise excitation at its top end in the surge direction. Riveros et al. [7] used a semi-empirical model to predict vortex-induced vibration response of a flexible riser and fitted auto-regressive (AR) models to detect and localize damage.

Although applications of both modal parameters and time series model based DSFs have been investigated for risers, comparison of the two has not been reported in the literature. In addition, realistic representation of ambient wave loading has not been addressed in simulations of the dynamic response of risers for virtual monitoring data generation. In this paper, natural frequencies and AR coefficients are identified from numerically simulated dynamic response of a riser to realistic ambient wave excitations and their damage sensitivities are compared for a series of damage extents.

In the following sections of the paper, the background theory is outlined for modelling of corrosion damage, simulation of dynamic response of the riser to ambient wave excitations, and hence generation of virtual monitoring data, and extraction of the natural frequencies and the AR coefficients from the response time series. Finally, damage sensitivity of the selected AR coefficients and natural frequencies are compared.

2. Theory

2.1 Modelling corrosion damage

Corrosion damage amounts to loss of cross-sectional area or reduced axial stiffness at the damaged region, which leads to loss of tension in a TTR as demonstrated in Dunbar et al. [8]. The schematics of healthy and damaged risers are given in Figure 1, where the top tension value T_{tu} at the undamaged state drops to T_{td} at the damaged state due to structural axial stiffness change from EA_{su} to EA_{sd} in the damaged region between $z = l_1$ and $z = l_2$. Note hereafter the subscripts u and d denote undamaged and damaged states, respectively.

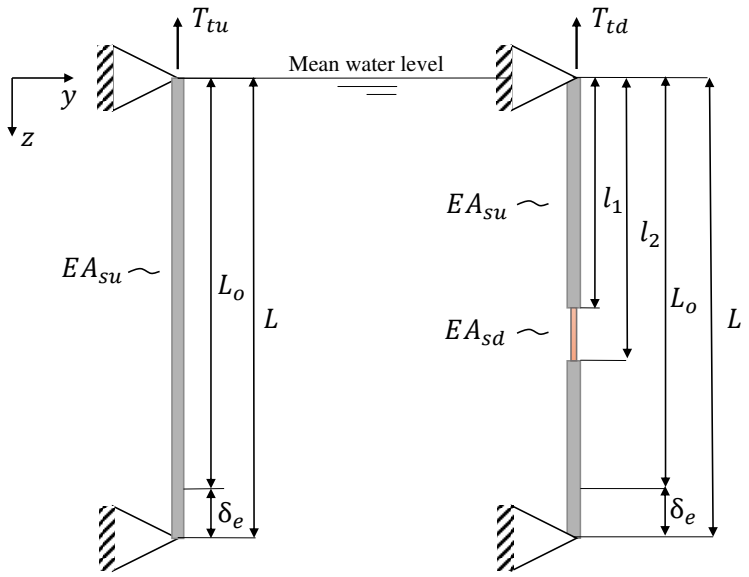

Figure 1. Schematics of a healthy (left) and a damaged (right) riser.

The reduced top tension, T_{td}, of a TTR due to corrosion damage can be expressed as [8]:

$$T_{td} = \frac{Q}{2(EA_{su} - EA_{sd})(l_2 - l_1) + 2EA_{sd}L_o} < T_{tu} \tag{1}$$

where

$$\begin{aligned} Q = {} & EA_{sd}(2T_{tu}L_o + 2w_{ed}(l_2 - l_1)(L_o - l_2) + w_{eu}(l_1^2 - l_2^2 + 2l_1(L_o - l_2))) \\ & + EA_{su}(l_2 - l_1)(w_{ed}(l_1 + l_2) + 2w_{eu}l_1) \end{aligned} \tag{2}$$

and $L_o = L - \delta_e$, in which L_o and L are the free and tensioned lengths of the riser, respectively, and δ_e is the elastic elongation due to the top tension. The effective weights per unit length of the riser at the undamaged and damaged regions are w_{eu} and w_{ed}, respectively, and are given as:

$$w_{eu} = (\rho_s A_{su} + \rho_i A_i - \rho_e A_{eu})g \tag{3}$$

$$w_{ed} = (\rho_s A_{sd} + \rho_i A_i - \rho_e A_{ed})g \tag{4}$$

The symbols ρ_s, ρ_i and ρ_e denote the densities of the structure and the internal and external fluids, respectively, and A_i and A_e are the internal and external cross-sectional areas, respectively. Since the corrosion damage in risers is predominantly external [2], this type of damage is considered here for the damaged states. Therefore, the internal cross-sectional area, A_i, remains the same for the undamaged and damaged states, whereas A_{eu} in the undamaged state drops to A_{ed} with damage.

2.2 Modelling ambient wave excitations

Risers are subject to environmental loads due to waves, currents and vessel motions, functional loads, such as internal and external pressure variations, and accidental loads due to ship impacts and tensioner failure. In this study, only wave loading is considered as the source of ambient excitation due to its persistence and ability to excite the riser globally. For a realistic representation of the energy density distribution of sea waves, the JONSWAP spectrum is used [9]:

$$S(\omega) = \alpha^* H_s^{\,2} \frac{\omega^{-5}}{\omega_p^{\,-4}} \exp\left(-1.25\left(\frac{\omega}{\omega_p}\right)^{-4}\right) \gamma^{\exp\left(-(\omega-\omega_p)^2 2\tau^2\omega_p^2\right)} \tag{5}$$

where S is spectral density, γ is the peak enhancement factor that depends on geographical sea location, ω is wave radial frequency, ω_p is spectral peak radial frequency, g is acceleration due to gravity, and τ and $\alpha^*$are given by:

$$\tau = \begin{cases} 0.07 & \omega \le \omega_p \\ 0.09 & \omega > \omega_p \end{cases} \quad \text{and} \quad \alpha^* = \frac{0.0624}{0.230 + 0.0336\gamma - 0.185(1.9+\gamma)^{-1}} \tag{6}$$

From a given energy density spectrum of the sea waves, it is possible to generate a time series wave profile to be used for the time domain dynamic response simulations. Dividing the spectrum into n=1…N discrete frequency components, for the nth discrete frequency value f_n, the corresponding wave height H_n can be obtained as [10]:

$$H_n = 2\sqrt{2 S_n \Delta_f} \tag{7}$$

where Δ_f is the frequency resolution of the spectrum and S_n is the nth spectral value. To each discrete frequency, a random phase angle, θ_n, distributed uniformly between 0 and 2π rad, is assigned. Finally, at the riser location, the free surface elevation, η, and horizontal water particle velocity, u, and acceleration, $\dot{u}$, are expressed in the time domain following linear wave theory with deep water approximation [10]:

$$\eta(t) = \sum_{n=1}^{N} \frac{H_n}{2} \cos(2\pi f_n t + \theta_n) \tag{8}$$

$$u(t,z) = \sum_{n=1}^{N} \pi H_n f_n e^{-k_n z} \cos(2\pi f_n t + \theta_n) \tag{9}$$

$$\dot{u}(t,z) = -\sum_{n=1}^{N} 2\pi^2 H_n f_n^{\,2} e^{-k_n z} \sin(2\pi f_n t + \theta_n) \tag{10}$$

Having determined the water particle velocities and accelerations from the JONSWAP spectrum, the inline hydrodynamic force is calculated from the linearized form of the Morison's equation [11]:

$$F_h(z,t) = \frac{1}{2}\rho_e D_o(z) C_d \sqrt{\frac{8}{\pi}}\sigma_{u_r}(z)\left(u(z,t) - \frac{\partial y(z,t)}{\partial t}\right) + C_m \frac{\pi}{4}\rho_e D_o^{\,2}(z)\frac{\partial u(z,t)}{\partial t} - (C_m - 1)\frac{\pi}{4}\rho_e D_o^{\,2}(z)\frac{\partial^2 y(z,t)}{\partial t^2} \quad (11)$$

where C_d is the drag coefficient, C_m is the inertia coefficient, D_o is the outer diameter of the riser, y is the transverse displacement of the riser, which is in-line with the wave direction, and σ_{u_r} is the standard deviation of the relative velocity, $u_r = u - \partial y/\partial t$. Eq. (11) states that the total wave-induced inline force on the riser consists of the drag force, inertia force, and added mass force, respectively.

2.3 Simulation of dynamic response of the riser

The partial differential equation of motion for a tubular segment of a TTR for small deflections is given by Kirk [12]. The equation can be extended for a damaged riser with pinned-pinned boundary conditions as:

$$m(z)\frac{\partial^2 y(z,t)}{\partial t^2} + \frac{\partial^2}{\partial z^2}\left(EI(z)\frac{\partial^2 y(z,t)}{\partial z^2}\right) - \frac{\partial}{\partial z}\left(\left(T_{td} - z w_e(z)\right)\frac{\partial y(z,t)}{\partial z}\right) = F_h(z,t) \quad (12)$$

where the total mass per unit length, m, the flexural rigidity, EI, and the effective weight per unit length, w_e, are described as piecewise functions due to presence of a damaged segment:

$$m(z) = \begin{cases} m_u, & 0 \le z < l_1, \\ m_d, & l_1 \le z < l_2 \\ m_u, & l_2 \le z \le L_o \end{cases} \quad EI(z) = \begin{cases} EI_u, & 0 \le z < l_1, \\ EI_d, & l_1 \le z < l_2 \\ EI_u, & l_2 \le z \le L_o \end{cases} \quad w_e(z) = \begin{cases} w_{eu}, & 0 \le z < l_1, \\ w_{ed}, & l_1 \le z < l_2 \\ w_{eu}, & l_2 \le z \le L_o \end{cases} \quad (13)$$

Substituting the hydrodynamic wave loading from equation (11) into the equation of motion (12) and rearranging the terms, the governing equation of motion can be expressed as:

$$m_t(z)\frac{\partial^2 y(z,t)}{\partial t^2} + \psi_D(z)\sigma_{u_r}(z)\frac{\partial y(z,t)}{\partial t} + \frac{\partial^2}{\partial z^2}\left(EI(z)\frac{\partial^2 y(z,t)}{\partial z^2}\right) - \frac{\partial}{\partial z}\left(\left(T_{td} - z w_e(z)\right)\frac{\partial y(z,t)}{\partial z}\right) = \psi_D(z)\sigma_{u_r}(z)u(z,t) + \psi_M(z)\frac{\partial u(z,t)}{\partial t} \quad (14)$$

where

$$
\begin{aligned}
m_t(z) &= m(z) + \psi_M(z) \\
\psi_M(z) &= (C_m - 1)\frac{\pi}{4}\rho_e D_o^2(z) \\
\psi_D(z) &= \frac{1}{2}\rho_e D_o(z) C_d \sqrt{8/\pi}
\end{aligned}
\tag{15}
$$

The solution to the partial differential equation of motion (14) is approximated by using the Galerkin method. To that end, a solution is assumed in the following form:

$$
y(z,t) = \sum_{i=1}^{N} \phi_i(z) q_i(t) \quad \text{with} \quad \phi_i = \sin(i\pi z / L) \tag{16}
$$

Substituting the assumed solution in the equation of motion and applying the Galerkin method yields a set of N ordinary differential equations as follows:

$$
\mathbf{M}\ddot{\mathbf{q}} + \mathbf{C}\dot{\mathbf{q}} + \mathbf{K}\mathbf{q} = \mathbf{Q} \tag{17}
$$

where the mass matrix, **M**, damping matrix, **C**, stiffness matrix, **K**, and excitation vector, **Q**, are given as:

$$
M_{ij} = \int_0^L m(z)\phi_i(z)\phi_j(z)dz \tag{18}
$$

$$
C_{ij} = \int_0^L \psi_D(z)\sigma_{u_r}(z)\phi_i(z)\phi_j(z)dz \tag{19}
$$

$$
K_{ij} = \int_0^L EI(z)\frac{d^4\phi_i(z)}{dz^4}\phi_j(z)dz + \int_0^L \left(T_{td} - zw_e(z)\right)\frac{d^2\phi_i(z)}{dz^2}\phi_j(z)dz + \int_0^L w_e\phi_i(z)\phi_j(z)dz \tag{20}
$$

$$
Q_j = \int_0^L \left(\psi_D(z)\sigma_{ur}(z)u(z) + \psi_M(z)\frac{\partial u(z,t)}{\partial t}\right)\phi_j(z)dz \tag{21}
$$

Having approximated the partial differential equation of motion as a set of N ordinary differential equations, time domain response of the riser to wave excitations was obtained in this study using the Newmark-β direct integration method [13].

2.4 Extraction of DSFs from virtual dynamic response of the riser

The time series of the simulated riser response to ambient wave excitations yields the virtual monitoring data, which is used for extraction of AR coefficients and natural frequencies. The AR model of the response can be expressed as:

$$
y(t) = a_1 y(t-1) + \ldots + a_p y(t-p) + e(t) \tag{22}
$$

where a_i, $i = 1,2 \ldots p$ are the AR coefficients, p is the model order and e(t) is the noise time series. The unknown AR coefficients are estimated here by using the Burg algorithm [14] and the optimal model order is determined using the Akaike information criterion

(AIC) [14]. The natural frequencies are identified from the power spectral density of the response by locating the dominant peaks in the spectrum, i.e., using the basic peak-picking approach [15], where the power spectral densities are calculated by using the Welch method [16].

3. Results

A series of simulations are performed for a reference structure whose characteristics are adapted from [12] and listed in Table 1. The JONSWAP spectrum, shown in Figure 2a, is defined with significant wave height $H_s = 8.7$ m, peak frequency $\omega_p = 0.5236$ rad/s and peak enhancement factor $\gamma = 3.3$. In total, a 128,000 s long water surface elevation and water particle velocity and acceleration time series is generated from the JONSWAP spectrum. Figure 2b shows an example 16,000 s long segment of the wave surface elevation time series.

Table 1. Properties of the reference TTR.

Parameter	Value	Parameter	Value
Inner diameter, D_i [m]	0.374	Density of structure, ρ_s[kg/m^3]	7840
Outer diameter, D_o [m]	0.406	Density of external fluid, ρ_e [kg/m^3]	1025
Length, L [m]	500	Density of internal fluid, ρ_i [kg/m^3]	920
Top tension, T_{tu} [kN]	1960	Drag coefficient, C_d	0.8
Elastic modulus, E [GPa]	210	Inertia coefficient, C_m	0.2

The response to wave excitations is obtained for the healthy state of the riser and for three different damage scenarios corresponding to 10, 20 and 30% cross-sectional area loss due to corrosion damage, respectively, which are affecting 15% of the riser length. The centre point of the damaged region is located at $z = L/5$. The generated acceleration response time series are divided into 8 segments to be used for identification of AR coefficients and natural frequencies. The number of comparison functions is selected as 15 for the Galerkin method. For the Newmark-β solution, the time step is set to 0.2 s and the coefficients are set to $\gamma = 1/2$ and $\beta = 1/4$, which corresponds to the assumption of constant acceleration between time steps.

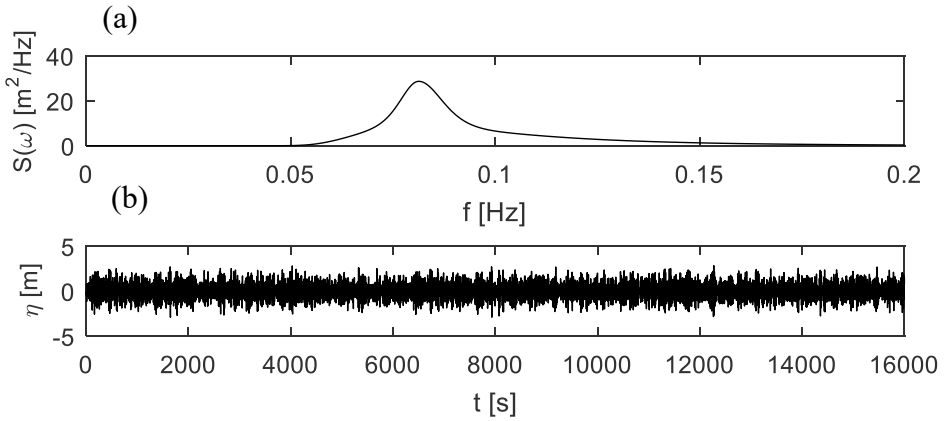

Figure 2. Simulation of wave loading: a) JONSWAP spectrum, and b) sample free surface elevation time history.

Figure 3 shows acceleration output power spectral densities of the riser at $z = L/10$ from one of eight 16,000 s long samples for the healthy and for the three damage scenarios. Note that no artificial 'measurement' noise was added to the generated response time series. For each acceleration response time series, the natural frequencies are identified from the peaks of these acceleration power spectral densities; the resulting mean values and standard deviations of the natural frequencies are given in Figure 4. The results show that the mean of the first natural frequency varies more significantly with increasing damage extent. However, in addition to the change in averages due to damage, a reliable comparison requires also corresponding variances to be considered as this gives an indication of state separability for noisy DSFs. To that end, the Fisher criterion is used here, which can be expressed as follows:

$$\mathrm{FC}(i) = \frac{\left(\overline{\omega}_{i,d} - \overline{\omega}_{i,u}\right)^2}{\sigma_{i,d}^2 + \sigma_{i,u}^2} \tag{23}$$

where $\overline{\omega}_i$ is the mean of the ith natural frequency, σ_i^2 is the corresponding variance and subscripts u and d denote, as previously, the undamaged and damaged states, respectively. Figure 5 shows the variation of the Fisher criterion with damage extents for the first four modes. Note the results were scaled such that the largest Fisher criterion is one. It follows from the figure that second natural frequency reaches the maximum Fisher criterion for 30% cross-sectional area loss due to damage and overall gives the highest Fisher criterion amongst all damage cases. Therefore, the second natural frequency is the most sensitive one within the first four natural frequencies for the selected damage location.

For AR modelling of the acceleration response time series, first the AR model order is determined using the AIC. Variation of the AIC with AR model order is given in Figure 6, which indicates that an AR model order 12 is appropriate for a satisfactory fit without using an excessively high number of terms.

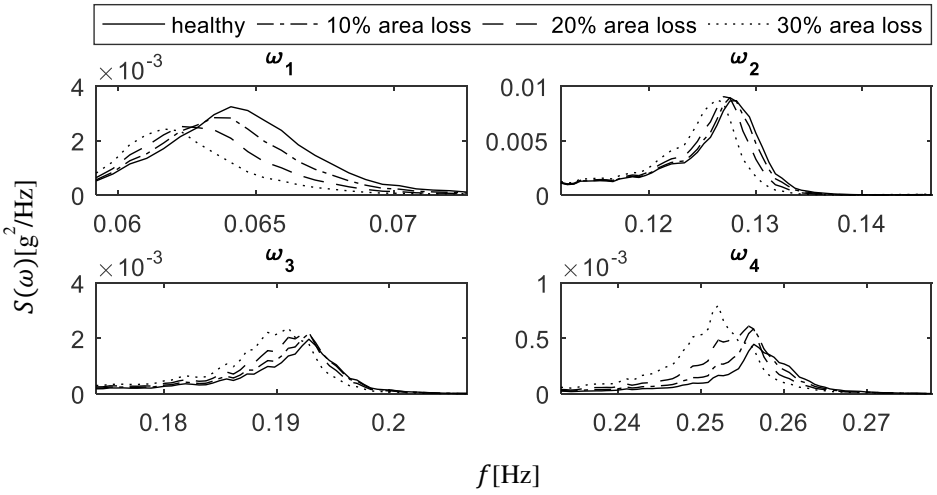

Figure 3. Power spectral density of the acceleration response in the neighbourhood of first four natural frequencies in healthy and damaged states.

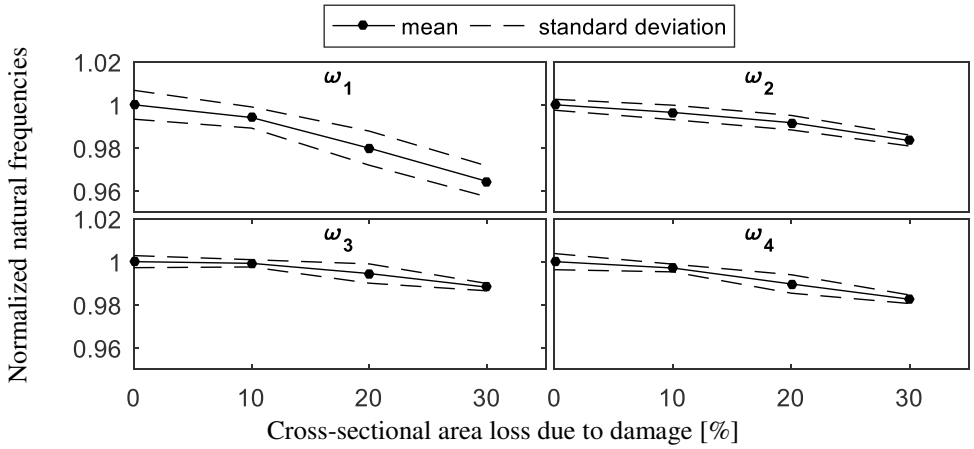

Figure 4. Damage sensitivity of natural frequencies.

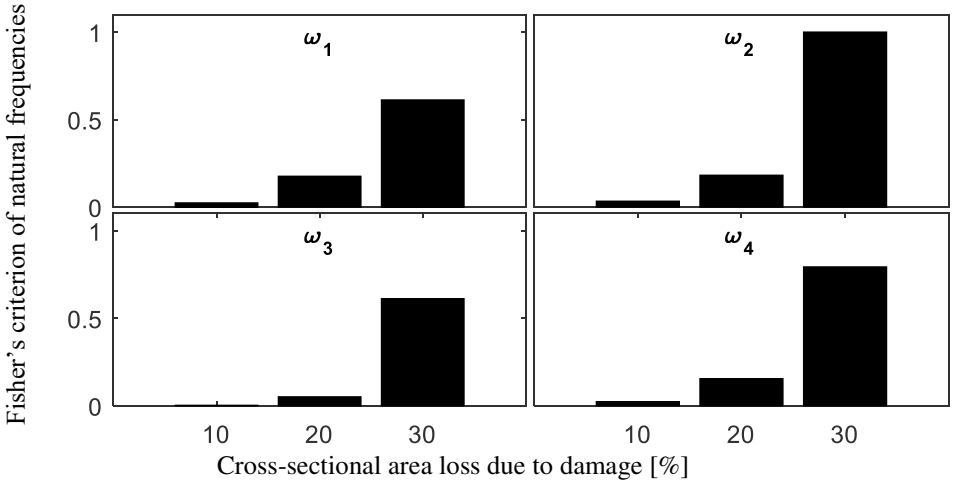

Figure 5. Variation of the Fisher criterion of the first four natural frequencies with damage extent.

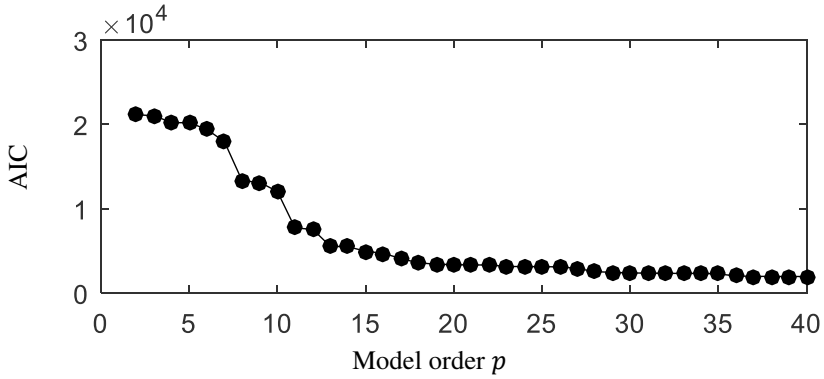

Figure 6. Variation of AIC with model order.

The sensitivity analysis performed for the AR coefficients is similar to the one applied for the natural frequencies. The mean values and corresponding standard deviations of AR coefficients are shown in Figure 7 for the selected damage scenarios. The Fisher criterion values for the AR coefficients are given in Figure 8, where the results are again divided by the overall maximum value. The comparison of the Fisher criteria indicates that the AR coefficient a_9 is the one most sensitive to damage.

Having selected features with the highest damage sensitivity (i.e. AR coefficient a_9 and the natural frequency ω_2), a comparison can now be made between the AR coefficients and natural frequencies as DSFs. Figure 9 shows that for the selected damage location and extents, the AR coefficient, a_9 is more sensitive to damage compared to the second natural frequency, ω_2 since it yields greater Fisher criterion values at all damage states.

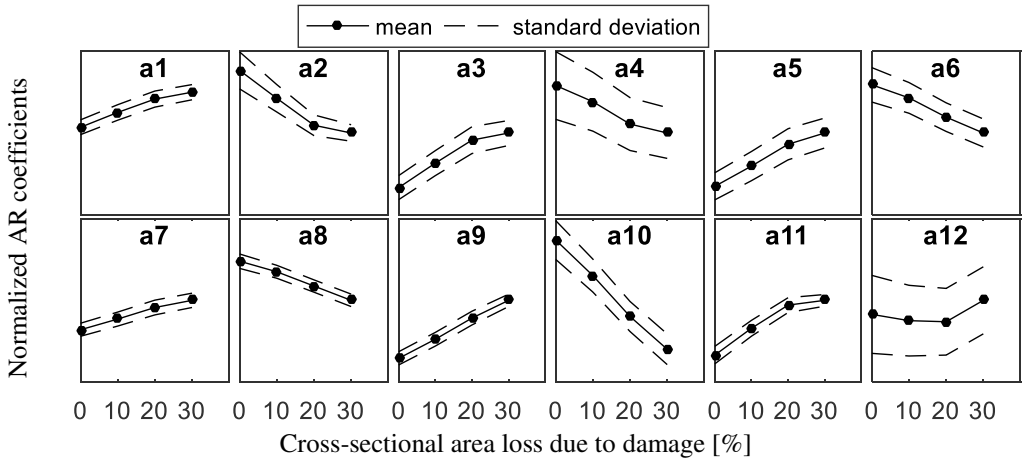

Figure 7. Damage sensitivity of AR coefficients.

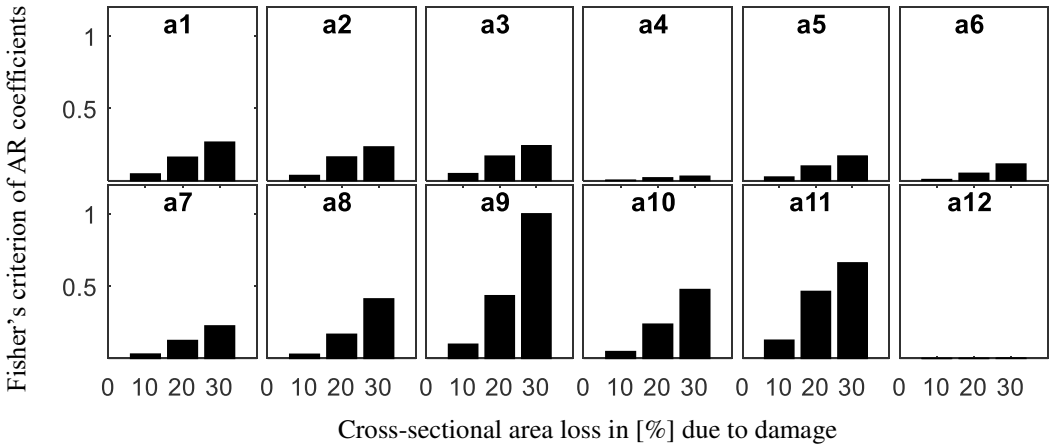

Figure 8. Variation of Fisher's criterion of AR coefficients with damage extents.

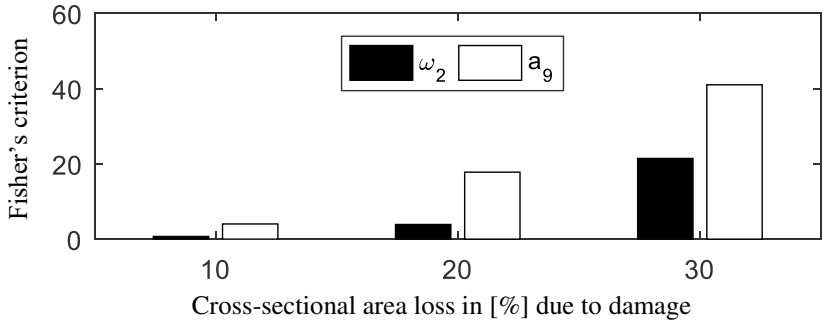

Figure 9. Comparison of variation of Fisher's criterion with damage extents for second natural frequency ω_2 and AR coefficient a_9.

4. Conclusions

In this paper, damage sensitivities of natural frequencies and AR coefficients were compared for vibration-based SHM of a TTR. Dynamic response of the riser to ambient wave excitations was simulated for a fixed damage location and a series of damage extents. The natural frequencies and the AR coefficients were identified from the resulting virtual monitoring data. The most sensitive natural frequency and the AR coefficient were selected from amongst the first four natural frequencies and 12 AR coefficients. The selected AR coefficient was shown to be more sensitive to damage compared to the selected natural frequency. However, sensitivity comparison of AR coefficients and natural frequencies might yield different results when damage location is changed, or results are influenced by measurement noise. Therefore, future work is aimed at addressing the influence of varying damage locations and noise levels on sensitivities of natural frequencies and AR coefficients, which will be supported through a series of laboratory wave flume experiments.

4. References

[1] M MacDonald, "PARLOC: 2001, The updated loss of containment data for offshore pipelines", Energy Institute, London 2003.

[2] M Lozev, R Smith and B Grimmett, "Evaluation of methods for detecting and monitoring of corrosion damage in risers", Journal of Pressure Vessel Technology 127(3), pp 244-254, 2005.

[3] X Zhou, D Wang, M Duan, J Gu and Y Liu, "Numerical study on mode curvature for damage detection of a drilling riser using transfer matrix technique", Applied Ocean Research 63, pp 65-75, 2017.

[4] C Huang and S Nagarajaiah, "Output-only structural health monitoring for deepwater risers: experimental study of wavelet modified SOBI and distributed force index algorithm", International Journal of Structural Stability and Dynamics 14(05), pp 1440010, 2014.

[5] C Bao, H Hao and Z Li, "Integrated ARMA model method for damage detection of subsea pipeline system", Engineering Structures 48, pp 176-192, 2013.

[6] H Liu, H Yang and F Liu, "Damage localization of marine risers using time series of vibration signals", Journal of Ocean University of China 13(5), pp 777-781, 2014.

[7] CA Riveros, T Utsunomiya, K Maeda and K Itoh, "Damage detection in flexible risers using statistical pattern recognition techniques", International Journal of Offshore and Polar Engineering 18(1), pp 35-42, 2008.

[8] D Dunbar, B Bayik, P Omenzetter and D van der A, "Experimental ambient vibration-based structural health monitoring in top-tensioned risers", SPIE Smart Structures and Materials + Nondestructive Evaluation and Health Monitoring, 13 pp, 2018.

[9] Y Goda, "A review of statistical interpretation of wave data", Report of the Port and Harbour Research Institute 8(1), pp 5-22, 1979.

[10] SK Chakrabarti, "Hydrodynamics of offshore structures", Computational Mechanics, Southampton, pp 439, 1987.

[11] LE Borgman, "Ocean wave simulation for engineering design", ASCE Journal of Waterways and Harbours Division 95(WW4), pp 557-583, 1969.

[12] CL Kirk, "Dynamic response of marine risers by single wave and spectral analysis methods", Applied Ocean Research 7(1), pp 2-13, 1985.

[13] NM Newmark, "A method of computation for structural dynamics", ASCE Journal of the Engineering Mechanics Division 85(3), pp 67-94, 1959.

[14] PJ Brockwell and RA Davis, "Time series: theory and methods", Springer Science & Business Media, pp 509, 2013.

[15] R Brincker and P Andersen, "Ambient response analysis modal analysis for large structures", Sixth International Congress on Sound and Vibration, pp 2549-2558, 1999.

[16] P Welch, "The use of fast Fourier transform for the estimation of power spectra: a method based on time averaging over short, modified periodograms", IEEE Transactions on Audio and Electroacoustics 15(2), pp 70-73, 1967.